ISSN: 2454-1907
DOI: https://doi.org/10.29121/ijetmr.v3.i4.2016.59

International Journal of Engineering Technologies and Management Research
A knowledge Repository
IJETMR

AN ACOUSTIC ANTIFOULING STUDY IN SEA ENVIRONMENT FOR SHIP HULLS USING ULTRASONIC GUIDED WAVES

Hossein Habibi [1], Tat-Hean Gan [*2], Matthew Legg [3], Ignacio Garcia de Carellan [4], Vassilios Kappatos [5], Vasileios Tzitzilonis [6], Cem Selcuk [7]
[1, *2, 3, 4, 5, 6, 7] Brunel Innovation Centre (BIC), Brunel University, Uxbridge, Middlesex, UB8 3PH, UNITED KINGDOM

Abstract:
Biofouling results in a range of adverse issues for ships and boats such as an increase in hydrodynamic drag force and fuel consumption and increased maintenance cost. To address this issue, toxic antifouling coatings have been developed. However, these toxic coatings can pose threats to marine life. This has led to research on less harmful techniques such as acoustic methods in the main implemented as laboratory trials. In fact, there have been relatively few sea trials and these are poorly documented. The current work has performed one of the few implemented field trials and the only one to be fully documented. In this sea trial, an optimised array of transducers generating ultrasound guided waves was attached to a hull representative plate in a port environment. The results of this work are evidenced by the significant reduction in-situ of a wide range of biofouling materials and organisms. The documented photographical evidence makes up for its scarcity in the published records of antifouling advances using acoustic techniques.

Keywords:
Biofouling, antifouling, sea trials, ultrasonic guided waves, ship hull.

Cite This Article: Hossein Habibi, Tat-Hean Gan, Matthew Legg, Ignacio Garcia de Carellan, Vassilios Kappatos, Vasileios Tzitzilonis, and Cem Selcuk, "AN ACOUSTIC ANTIFOULING STUDY IN SEA ENVIRONMENT FOR SHIP HULLS USING ULTRASONIC GUIDED WAVES" *International Journal of Engineering Technologies and Management Research*, Vol. 3, No. 4(2016)14-30.

1. INTRODUCTION

1.1.BIOFOULING CONSEQUENCES FOR UNDERWATER, MAN-MADE SURFACES

Biofouling is the adhesion, growth and reproduction of biological materials and living organisms on artificial surfaces, such as ship hulls, in a marine environment. It has two main components: microfouling, which is the formation of a biofilm and adhesion surface; and macrofouling, which is the attachment of larger organisms such as barnacles, seaweed, mussels, and diatoms [1]. Microfouling usually appears within seconds on a ship's hull after it is immersed in the sea water [2].

The effects of biofouling can be very problematic for underwater structures especially ship hulls and submarines. The marine industry spends billions of dollars worldwide in the prevention and removal of marine fouling. Without using a protective system against marine fouling deposits, it takes only 6 months that fuel consumption in ships raises up to 40% due to increased hydrodynamic drag [3]. For example, heavy calcareous fouling is calculated to increase parasitic shaft torque by 86% in comparison with a hydraulically smooth hull at cruising speed [4]. The more torque needed from the engine, the more fuel is consumed and the more environmental contamination may occur. Higher rates of corrosion are another major concern with biofouling. A hull protective coating may be damaged due to biological reactions, which makes the hull surface more vulnerable to seawater corrosion [5]. As a result, the structural integrity of the ship's hull is compromised sooner. Another consequence of biofouling is the increase in costs and loss of operation time for maintenance. Moreover, the substances generally used in the current cleaning processes are usually toxic and released in the sea [6].

1.2.ANTIFOULING TECHNIQUES AND ASSOCIATED DRAWBACKS

Biofouling is a significant issue in the marine field, as described above. There has therefore been considerable interest and attention paid to developing an efficient, environmentally safe antifouling strategy. Until now a wide range of technologies to control biofouling has been attempted. A common technique is the use of antifouling toxic coatings. One of these coatings, for example, included Tributyltin (TBT) compounds and was used worldwide, reaching almost 70% usage of world voyages [7, 8]. This substance was extremely toxic to marine life and has now been banned.

A non-toxic alternative against fouling uses acoustic methods. These techniques use transducers emitting mechanical waves with operating frequencies ranging from audible (20Hz – 20 kHz) to ultrasonic (above 20 kHz) frequencies. Multiple transducers can be used cooperatively to form an array that optimises antifouling performance. The topology of arrays is of high importance due to the effects of nodes and anti-nodes, which cause destructive and constructive interference respectively at different positions in the interference pattern. Transmission frequency is another important factor as the change in frequency can change the magnitude and dominant direction of vibrations and also the position of the antinodes which then degrades the effectiveness of antifouling [9]. One of the main problems is that the efficacy of acoustic biofouling prevention decreases with distance from the transducer as the waves are attenuated as they propagate [10].

A number of studies have been carried out using high power ultrasound waves leading to strong cavitation that kills barnacles. In research conducted by Kitamura et al. (1995), the optimum cleaning frequency of 19.5 kHz resulted in 50% barnacle larvae mortality [11]. In addition, there is considerable concern associated with the negative effects of man-made noise on marine life. Sound plays a key role for many marine species to navigate and communicate [12]. There is a number of studies carried out within the audio frequency range. Some have reported successful results in inhibiting barnacle settlement in laboratory studies within a low frequency range between 17 Hz and 445 Hz [13, 14]. However, the audible acoustic techniques can cause *hearing mask* on some life forms if the noise is within their hearing range. It means that the auditory tissue of the life form may become incapable of detecting biologically relevant sounds in its environment [15]. Furthermore, some studies have reported that the audio sound emitted by ships

and vessels especially between 30 Hz and 2 kHz can attract fouling and cause faster growth of biofouling rather than deterring it [12, 16].

Regarding the power commonly consumed by these techniques, Mazue et al. (2011), for example, were able to remove biofouler and other foulers on a boat through ultrasonic transducers operating at 20 kHz with 1000 W power consumption [9]. Bott (2000) also used a piezoelectric transducer with a frequency of 20 kHz and power consumption of 600 W at three 30-sec treatment intervals per day to remove algae and fungi from a heat exchanger tube [17].

Finally, it should be noted that many of the studies carried out so far, are within small-scale laboratory environments with single species. Legg et al. (2015) in a comprehensive review has discussed and concluded that more photographically documented trials need to be performed to work out the optimum operational factors and practical conditions of use of an efficient and environmentally safe acoustic anti-biofouling system for a wide range of fouling organisms [18]. In fact, it has been extensively reported that the acoustic-based strategies and technologies for fouling prevention and removal, applied on ships, vessels and docks, are needed to be improved. To this end, final experiments were carried out as field trials in port rather than on limited lab-scale experiments for specific life forms. Results are presented and evidenced with in-situ photographs taken at appropriate time intervals.

In the following section, a brief introduction on the Ultrasonic Guided Waves (UGW) and its background as a deterrent to the accretion of undesired material on surfaces is presented. Then the approach adopted in the current work and the experimental characterisation of key parameters such as operating frequency, wave mode, and optimal transducer array geometry will be demonstrated. Finally the experimental setup with the results of sea trials will be presented.

1.3.ULTRASONIC GUIDED WAVES

Ultrasonic guided waves (UGW) are waves travelling through bounded structures within a frequency range beyond the human audible range (normally > 20 kHz) and are widely used in Non-Destructive Testing (NDT). According to wave propagation theory, propagation of UGW induces displacements and stresses inside a structure which leads to appearing a large number of oscillation modes [19]. Most wave properties depend on the mode of the propagating wave. Hence, selecting the proper UGW mode and the right frequency can generate appropriate displacements on structure's surface which protects against unfavourable accretion of materials such as biofouling, ice or industrial dirt. The selection of appropriate modes not only makes the wave *guided* to a target for specific purposes but unlike conventional unguided ultrasound waves, it provides long range coverage of structures with low attenuation.

In conventional ultrasound techniques, waves propagate as bulk waves. Bulk waves can be in the form of compression or shear movement of particles in the medium. They usually travel with constant velocity and the pulses are launched with a wide frequency spectrum. Conversely, an UGW can be defined as an acoustic wave transmitted via a process that limits physical dispersion along the propagation direction. The pulses are launched with a narrow frequency spectrum. Guided waves' velocities vary with frequency, thickness of the structure and wave mode. The wave modes are asymmetric and symmetric longitudinal, flexural and torsional. One

ISSN: 2454-1907
Impact Factor: 1.745 (I2OR)

of the important steps in this study has been to determine appropriate wave modes and to select the most effective transducer array for a particular ship hull thickness, as explained in detail later.

The proposed biofouling prevention system uses UGW with power levels low enough not to generate cavitation, which might kill life forms. It aims to propagate waves appropriately, distribute energy uniformly and generate interface displacements. As the UGWs propagate through structures and reach boundaries, the transmitted and reflected waves interfere to attain a steady state vibration with the potential to prevent accumulation or growth of fouling types on submerged surfaces.

2. EXPERIMENTAL DEVELOPMENT

2.1.OVERALL APPROACH

This work is a documented investigation into the control of marine biofouling using UGW and the development of an acoustic fouling prevention. The system consists of an ultrasound generator and a transducer array, as shown in the Fig.1. This schematic represents the experimental configuration including the transducer array and the components used in the ultrasound generator. It also illustrates the details of a system used to attach single transducers in the array, comprising transducer, structure for housing the transducer and coupling agent.

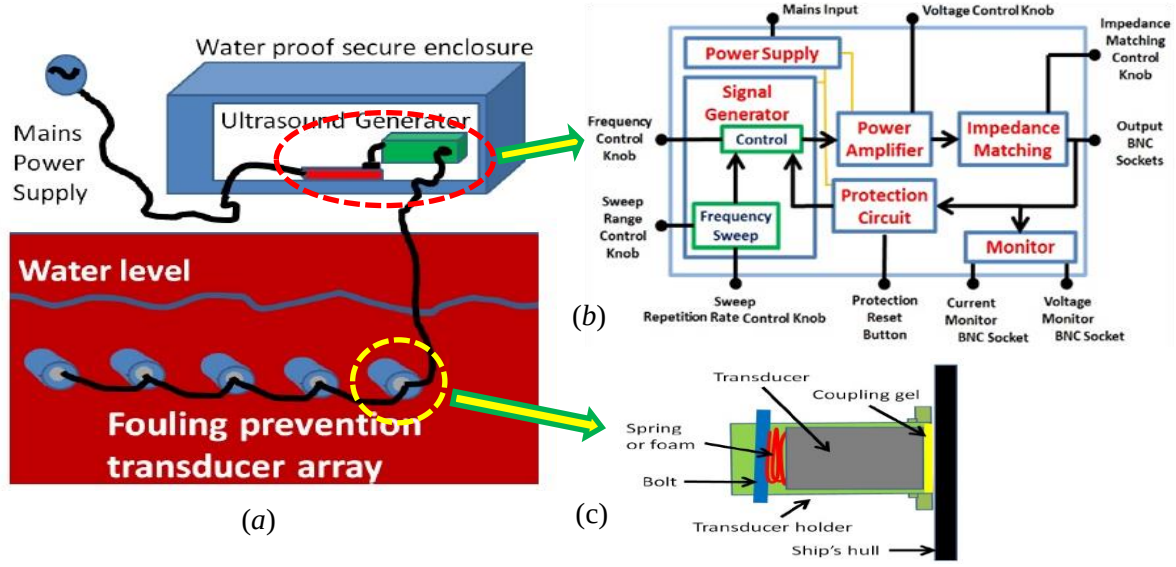

Figure 1: *a*) Proposed antifouling approach for a ship hull representative plate. *b*) Block diagram showing ultrasound generator components; *c*) Attachment system for a single transducer

To explore this concept, impedance analysis was first carried out for the transducers, followed by vibrometry analysis to validate the impedance analysis results and to characterise the appropriate magnitude and direction for antifouling vibrations. Moreover, vibrometry results evaluated the energy propagation on the contact surface of the transducers at the selected frequencies. In the following, dispersion curve and wave mode analyses following the principles of UGW were performed to determine the best excitation wave mode and the geometrical arrangement of the

ISSN: 2454-1907
Impact Factor: 1.745 (I2OR)

transducer array that most efficiently deliver distributed energy over the ship hull represented by the test plate. Finally, the plate was immersed in sea water in a port and the results were monitored photographically.

2.2.DESIGN OF ULTRASOUND GENERATOR

To drive the cleaning transducers, an ultrasound generator was developed. As seen in Fig. 1*b*, the generator is composed of four key parts; a signal generator, power amplifier, impedance matching circuit, and protection circuit. The maximum power is about 300 W. High voltages are achievable using this hardware since it runs from the mains supply and uses a step-up transformer. In practice, however, it is operated well below the maximum output level. The photographs displayed in Fig. 2 illustrate the developed generator (a), and the antifouling approach (b) for a successful application.

(a)

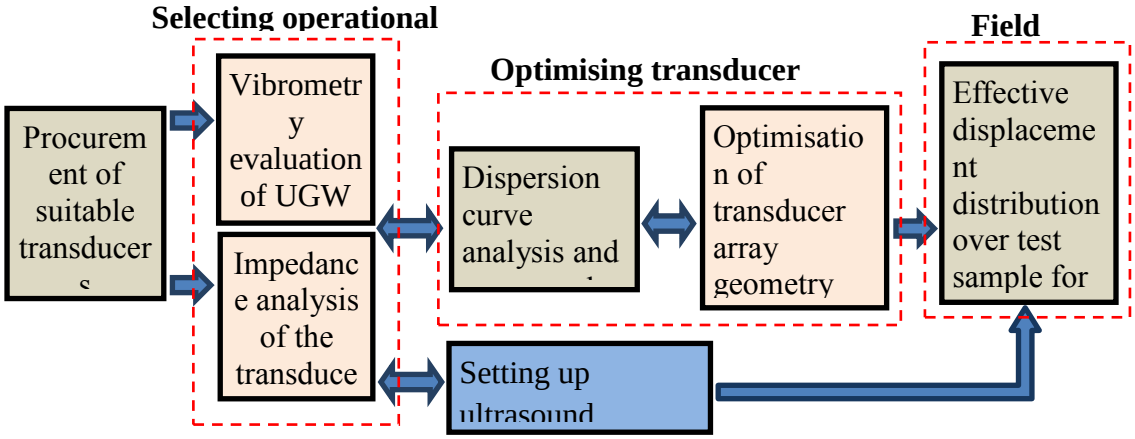

(b)

Figure 2: Photograph of the developed ultrasound generator (a), Diagram of the antifouling approach (b).

2.2.1. SIGNAL GENERATOR

A key part of the signal generator is the pulse width modulator chip. This generates square wave waveforms. The frequency of the output waveform may be adjusted by changing the value of a timing capacitor and resistor. In this case, the capacitor has been kept constant and the resistance is varied using a potentiometer as a variable resistance. The ability to generate a frequency sweep is a useful feature as it potentially prevents the formation of null points due to effects such as the interference of transmitted and reflected waves. The frequency sweep also reduces the possibility

of overloading the system due to the low impedance of the transducers at their resonance frequency. A frequency sweep may be implemented by varying the voltage across the frequency control resistor with time, using a frequency sweep circuit. The sweep range and repetition rate are adjusted using two potentiometers.

2.2.2. POWER AMPLIFIER

A power amplifier circuit is used to convert the logic voltage level waveform from the signal generator into a high-power, square waveform.

2.2.3. IMPEDANCE MATCHING

A voltage step-up transformer provides increased voltage and provides some impedance matching for the transducers. This can be varied between three levels using a control knob.

2.2.4. VOLTAGE AND CURRENT PROTECTION

Ultrasound cleaning transducers exhibit resonance frequencies where they have maximum gain. At these resonances, the voltage and current levels can become large potentially causing damage to the generator so a protection circuit using a step-down voltage and current transformer and a bridge rectifier circuit is used which converts the output AC voltage and current waveforms into DC voltages. The DC voltage level is compared to a reference voltage level. If the DC voltages go above the reference, a shutdown signal is sent to the signal generator. Initially this required a reset button to be pressed if the protection circuit was tripped but an auto reset feature has now been implemented that resets the protection circuit about 10 seconds after the protection circuit has engaged.

2.2.5. MONITORING OUTPUTS

The output voltage and current may be too large to be safely monitored directly using a standard oscilloscope. Two isolated monitoring outputs are, therefore, included. These use voltage and current step-down transformers to convert the output waveform into low voltage waveforms that can be safely monitored on an oscilloscope.

2.3.CHARACTERISATION OF VIBRATION OF PLATES WITH TRANSDUCERS ATTACHED

The transducer array was encapsulated in a waterproof casing. An attachment system composed of a pipe, flange, spring (or foam) and bolt has been used to house the waterproofed transducer unit. See Fig. 1(c) for details.

Two types of high power ultrasonic transducers developed by Sofchem for use in fouling cleaning of small ship hulls were provided to be studied in this work. These transducers were studied and analysed to deliver optimal vibrations with highest normal-to-plane amplitude. As mentioned above, the aim of this approach is not the generation of high levels of sound pressure leading to cavitation, rather it relies on maximising the displacement of the ship hull substrate.

ISSN: 2454-1907
Impact Factor: 1.745 (I2OR)

2.3.1. IMPEDANCE ANALYSIS

Ultrasound cleaning transducers have narrow frequency bands where they operate efficiently. These bands show up as minimum points in a transducer's electrical impedance. It is important to measure this impedance to assist in the design of the generator hardware, such as the ultrasound generator impedance matching circuit, and also to identify the optimum operating frequencies. The resonance frequencies and impedance of the transducers may be measured using an impedance analyser. Mechanical impedance is a measure of how much a structure resists motion when subjected to a given force. It relates forces to velocities acting on a mechanical system. A transducer is a device that converts electrical energy to mechanical energy and vice versa. Therefore, impedance analysis can be used to find the resonance frequencies of a mechanical system where the displacement of the transducer should be higher. These frequencies should correspond to maximum prevention of biofouling.

Piezoelectric transducers have been modelled using an equivalent circuit [20]. They have complex input impedance which affects their driving response, bandwidth, sensitivity and power output. It is therefore convenient to approximate the ultrasonic transducer by an electrical model shown in Fig. 3.

Both capacitance and inductance, determine the imaginary component of the impedance

$$Z = R + jX \tag{1}$$

where Z is the impedance; the resistivity R is the real part, and jX is its imaginary part. At resonance the magnitude of the impedance is at a minima and the phase between the voltage and the current changes from approximately -90 degrees to +90 degrees. At resonance, a large fraction of the electrical energy is converted to mechanical energy. Impedance analysis can find the resonance frequencies of a transducer where the highest displacements occur and also gives information about the voltage and current needed by the transducer at each frequency.

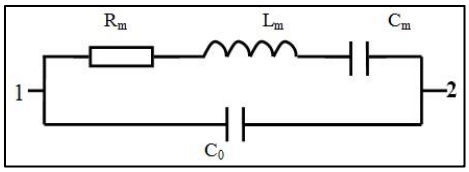

Figure 3: Illustration of the electronic equivalent circuit model of a common piezoelectric transducer. C_0 is the electrical capacitance of the transducer and L_m, C_m, and R_m describe the resonance mechanical properties of the transducer.

Four piezoelectric transducers were obtained from Sofchem and their characterisation was performed as part of the development process. Table 1 lists the transducers and their specifications in use for fouling removal.

Table 1: Physical properties of selected Sofchem transducers

Transducer No.	**Length (mm)**	**Diameter (mm)**	**First resonance frequency (kHz)**
1& 2	55	56	23
3& 4	95	56	45

ISSN: 2454-1907
Impact Factor: 1.745 (I2OR)

Each piezoelectric transducer was connected to the impedance analyser which generated a frequency sweep between 1 kHz and 100 kHz at constant voltage amplitude while measuring the impedance, transmittance and phase of the circuit at each frequency to be used for the design of generator impedance matching circuit. The measured impedance is shown in Figs. 4*a* and 4*b*. It can be seen that each transducer has different resonance frequencies. The occurring resonance frequencies are related to the dimensions and materials of the horn of the transducer and the casing. Figure 4*a* indicates that the transducers 1 and 2 have the first minimum about 23 kHz. This minimum has a double peak likely due to the encapsulation which may affect the resonance frequency of the whole system. Transducers 3 and 4 have a first resonance frequency about 45 kHz; see Fig.4*b*. In this case, a pronounced minimum impedance can be seen.

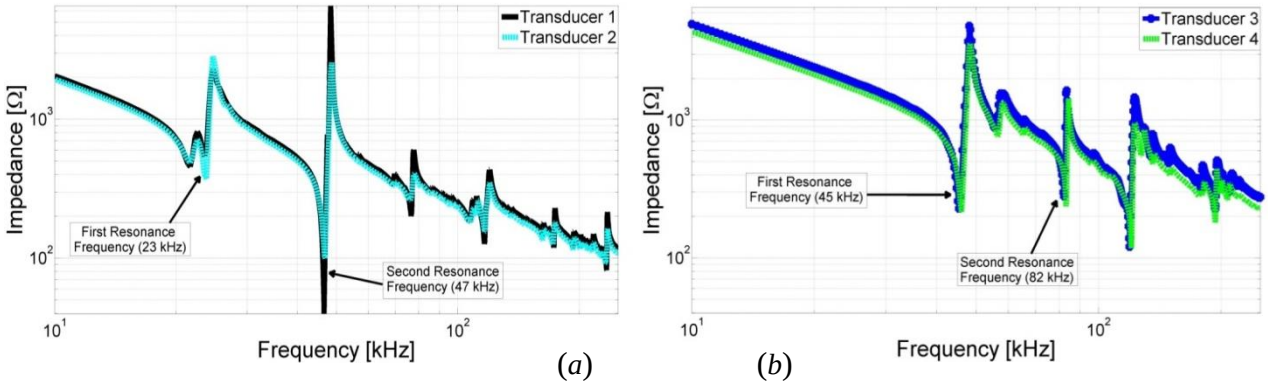

Figure 4: Impedance analysis of the transducers; *a*) transducers 1&2, *b*) transducers 3&4

The first resonance frequency of transducers 3 and 4 are very close to the second resonance frequency of transducers 1 and 2. Potentially transducer 2 could be used to generate both frequencies which could eliminate the need for transducers 3 and 4 provided that it could generate displacements larger than transducer 3.

2.3.2. VIBROMETRY ANALYSIS

The impedance analysis gives an indication of the resonance frequencies of a transducer. However, this does not give an indication of how efficient the transducer is at converting a voltage waveform into a mechanical waveform. For example, different sections of the transducer head may be moving in opposite directions causing low transfer of mechanical energy to a ship's hull. In addition, the operating frequency to be chosen should resonate most efficiently in the direction Z indicated in Fig. 5*b*. It is, therefore, important to measure the physical displacement across the total surface of the transducer head. This measurement was carried out using a laser scanning vibrometer. Figure 5*a* presents a photograph of the vibrometer experimental setup and Fig.5*b* shows one of the transducers (No. 2) being tested in this experiment. A Polytec PSV-400 laser scanning vibrometer and Teletest pulser receiver system were used for these experiments. The piezoelectric transducers were connected to the Teletest system and a periodic chirp (wide frequency band) produced. The vibrometer laser heads detects the displacements at each frequency.

ISSN: 2454-1907
Impact Factor: 1.745 (I2OR)

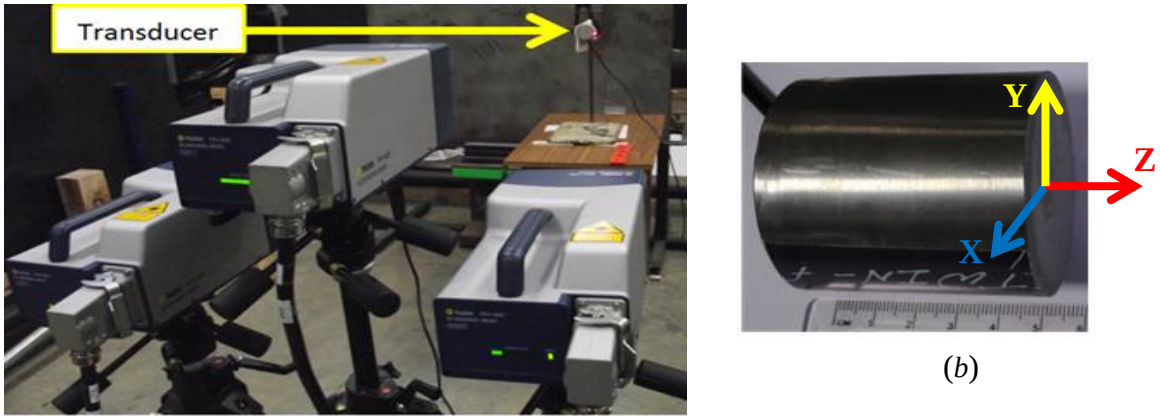

(*a*) (*b*)

Figure 5: Photo (*a*) shows the vibrometer experimental setup for transducer characterisation; Photo (*b*) shows transducer 2 with arrows drawn on to indicating the reference frame used in the scanning vibrometer measurements. The z-axis points out from the centre of the transducer head while the x and y-axis lie in the plane of the transducer head.

The scanning vibrometer analyses the results as an FFT (Fast Fourier Transform) or time and plot of the actual vibration of the analysed surface as a function of time or frequency. It resolves the displacement, velocity, or acceleration of the surface into X, Y, and Z axis components (refer to Fig.5*b*).

Figures 6*a* and 6*b* present examples of the actual vibration of transducer 2 for two different frequencies in colour spectra. In Fig.6*a*, it can be observed that, at 47 kHz, the majority of the contact surface of the transducer vibrates simultaneously. In contrast, at 56.3 kHz, as shown in Fig.6b, the entire transducer surface is not vibrating simultaneously which means the transducer would not be able to deliver maximum power through uniform wave propagation to cover the areas evenly. In other words, this effect would degrade the uniformity of energy distribution over the target area.

Another important factor is the magnitude and direction of the displacements induced by the transducers. The displacement of the contact surface of the transducer in the x, y and z directions, can be seen in Figs. 7*a* and *b* for transducers 2 and 3 respectively. In both transducers, the displacement in the Z axis was much higher than the displacement in the other two axes due to the compression waves produced by transducers at this mode.

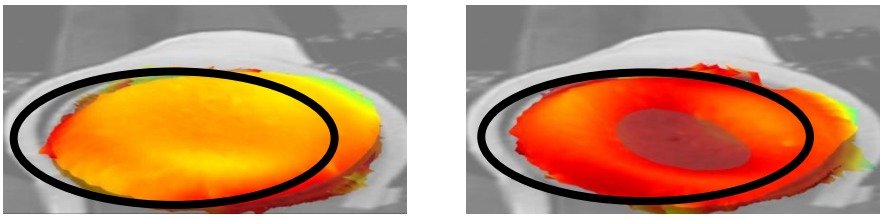

(*a*) (*b*)

Figure 6: Contact surface vibration of a sample transducer for two different frequencies; *a*) f = 47 KHz, *b*) f = 56.3 KHz. A black ring has been drawn over the image to roughly indicate the edge of the transducer head.

ISSN: 2454-1907
Impact Factor: 1.745 (I2OR)

Also, comparing the two figures shows that transducer 2 produces higher displacements than transducer 3. In transducer 3, according to Fig. 7*b*, the displacement at 82.3 kHz is much larger than the displacement at the first resonance frequency. However since the displacement amplitude due to excitation of the second resonance of the transducer 2 (at f = 47 kHz) is bigger than those of transducer 3, it is again inferred that transducer 2 at the operating frequency of 47 KHz is a more appropriate choice. It is worth mentioning that the displacement amplitude was increased by about 4000 times using the developed high-voltage input generator in place of the available Teletest system. The displacements due to excitation of some frequencies above 100 kHz are also high. However, the modes above 100 kHz are dispersive which is not favourable as will be described in the next section.

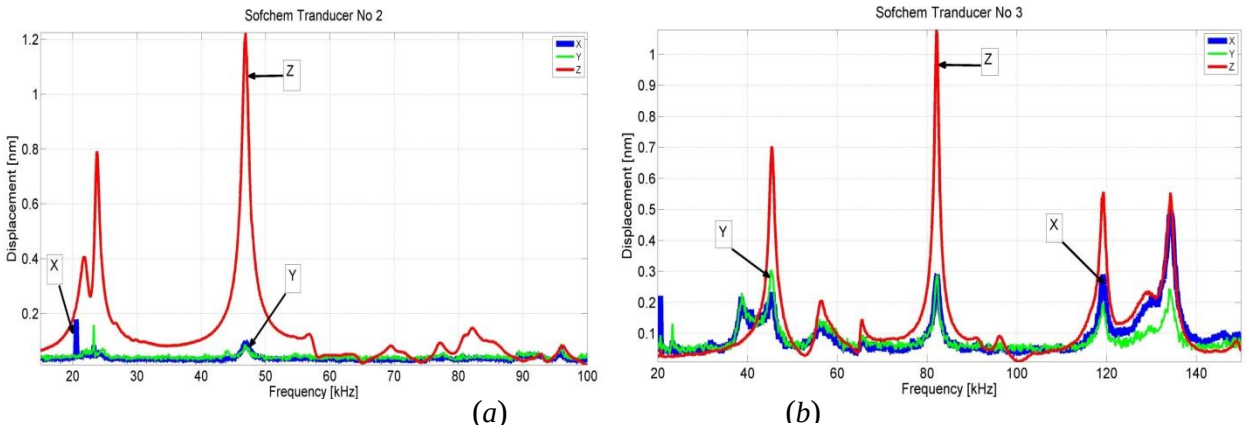

(*a*) (*b*)

Figure 7: Displacements in the X, Y and Z-axis of *a*) transducer 2, *b*) transducer 3, as a function of frequency

Also, note that the results of the experiments obtained by both the impedance analyser plot in Figs. 4 and the scanning vibrometer presented in Figs. 7match closely as expected. In other words, both Fig. 4a and Fig. 7a indicate the resonances occurring at 23 kHz and 47 kHz. Similarly, Fig. 4b and Fig. 7b show the resonances at 45 kHz and 82 kHz.

2.3.3. TRANSDUCER PAIR MEASUREMENTS

The geometrical arrangement of the transducers on the ship hull is of high importance as it can significantly affect the wave propagation and power concentration. It is logical to assume that higher displacements of the plate, particularly in the Z direction shown at Fig. 5*b*, provides higher cleaning efficacy. One of the main factors affecting the displacement of a vibrating plate is the geometry of the transducer array. In this work, the selection of frequency, wave mode, interference considerations and the location of the transducers have been investigated.

Perhaps the most important difference between conventional ultrasonic and guided waves is the dispersion phenomenon. Dispersion is the change in velocity of a guided wave with change of frequency. The dispersion curves change with the wall thickness of the propagation media which is an important factor to be considered in the transducers' location because it would influence the energy distribution and attenuation over the plate.

ISSN: 2454-1907
Impact Factor: 1.745 (I2OR)

Figure 8 shows an example of a guided wave dispersion curve of a steel plate of 1.5 mm thickness that plots the phase velocity of each wave mode against the frequency.

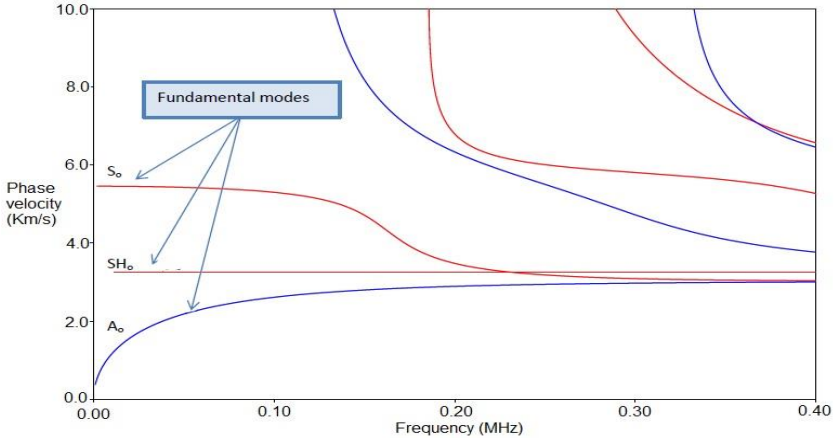

Figure 8: Dispersion curves for a steel plate of 1.5 mm thickness

These dispersion curves are considered to find the best way to vibrate the ship hull plates. As can be seen in Fig. 8, only three modes exist below 100 kHz. These modes are the fundamental modes and are always generated when a plate is vibrated. The selection of wave modes is done first by looking for a region without dispersion (no change in velocity as the frequency changes) and with a minimal number of modes to ensure that the energy is not dispersed. The A_0 mode has higher out-planed displacement. This would appear to be a suitable wave mode to excite as the aim is to look for a mode generating the highest displacements. In addition, Fig. 8 indicates that frequencies above 100 kHz cannot be of interest because of the higher number of vibration modes and thus dispersion excited above that frequency.

The other important factor to be considered in the array arrangement is interference of waves. Two waves can be superimposed to form a resultant wave of greater or lower amplitude. Constructive superposition should be used to ensure the highest displacement in the hull plate. The interference of two waves of equal frequency and phase which are placed at a multiple of half the wave length, λ/2, away from each other can create a constructive interference.

The wavelength can be obtained through $v = f.\lambda$ while the velocity 'v' is determined from the dispersion curves, Fig. 8.

The wavelength can be calculated for any ship hull if the dispersion curves are provided. The location of the transducers will be then determined. As an example, Table 2 shows the values obtained for the three fundamental waves using the dispersion curves working out through the equation $v = f.\lambda$ at f = 47 kHz which was already identified as the best frequency.

Table 2: Wave parameters obtained through the dispersion curves displayed in Fig. 8

Mode	v (m/s)	f (kHz)	λ (mm)
A_0	2208	47	47
SH_0	3405	47	72
S_0	5676	47	121

ISSN: 2454-1907
Impact Factor: 1.745 (I2OR)

Among the three fundamental modes, the shear horizontal wave mode (SH_0) causes only in-plane displacement which therefore is not of interest. Regarding the other two modes, some preliminary experiments showed that excitation of asymmetric modes (A_0) cause displacements of higher amplitude than symmetric (S_0).

To demonstrate this possibility for generating constructive interference, a number of experiments were carried out using two transducers, numbered 1 and 2 in Table 1, at the excitation frequency of 47 kHz. The experiment was carried out through 6 different setups. It is noted that if the wavelength is shorter than the transducer diameter, any multiple of λ/2 has the same effect. For this reason, the transducers have been located in positions at 3λ/2 of the A_0 mode, and for comparison also the S_0 mode, on a 2000mm x 1000mm x 1.5mm steel plate. For each setup, a frequency sweep between 40 kHz and 50 kHz was performed in the transmission area with different transmitting configuration. The distance between transducers and the orientation relative to the transmission area were varied. The transmitting transducers were arranged horizontally, vertically and diagonally, each tested for both A_0 and S_0 mode wavelengths. The reception area has four sensors located randomly to measure the amount of energy received at each location. The positions of the four sensors were fixed as displayed in the general layout in Fig. 9b.

The signals received in the reception area were processed and analysed to understand the effects of wave propagation. A photograph taken from one of the test configurations is shown in Fig. 9a. Likewise, Fig. 9b represents the general layout of the experiment with detailed dimensions.

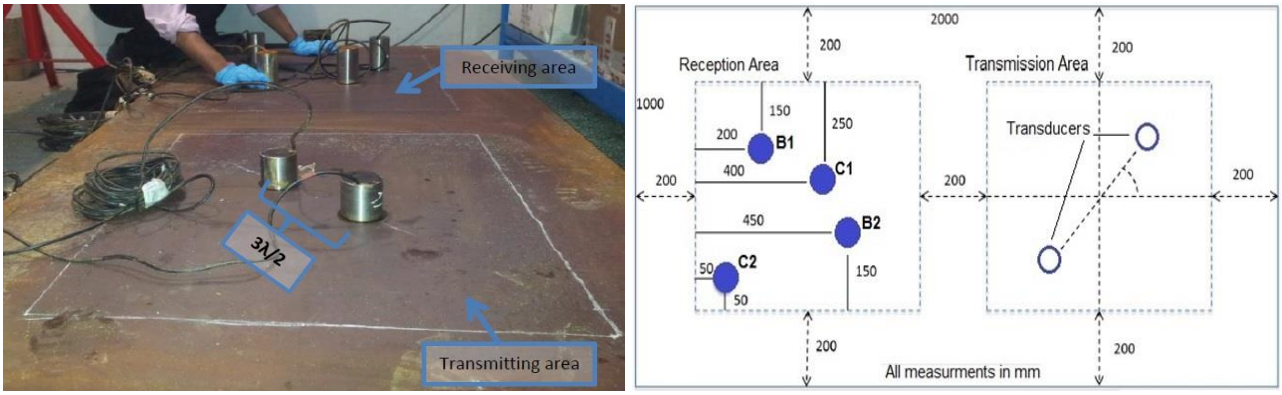

(*a*) (*b*)

Figure 9: *a*) Lab experimental set-up for characterising wave modes and the transducer array at f=47 kHz; *b*) Dimensional details of the general layout of the experiment.

3. FIELD TRIAL RESULTS

The efficiency of the developed approach was evaluated using a test plate in a real marine environment, where different types of fouling such as algae, fungi and barnacles were present. Final trial took place at Vlissingen in the Netherlands. The site was a port environment. It was a secured place with limited access to public and near to the offices of a CleanShip consortium member which was very helpful in case an onsite inspection was needed.

ISSN: 2454-1907
Impact Factor: 1.745 (I2OR)

The idea of the experiment was to immerse two plates into water; one with the transducers attached on (test plate) and one (a steel plate) to which no transducer was attached, used only as a control for the test plate. The test plate setup as displayed in Fig. 10*a* was a steel 2m x 1m x 0.0015m plate, painted for corrosion protection on which four high power ultrasonic transducers were mounted. Two of these transducers were operated as the main ones and the other two played a backup role in the case of any failure. The control plate is also shown in Fig.10b.

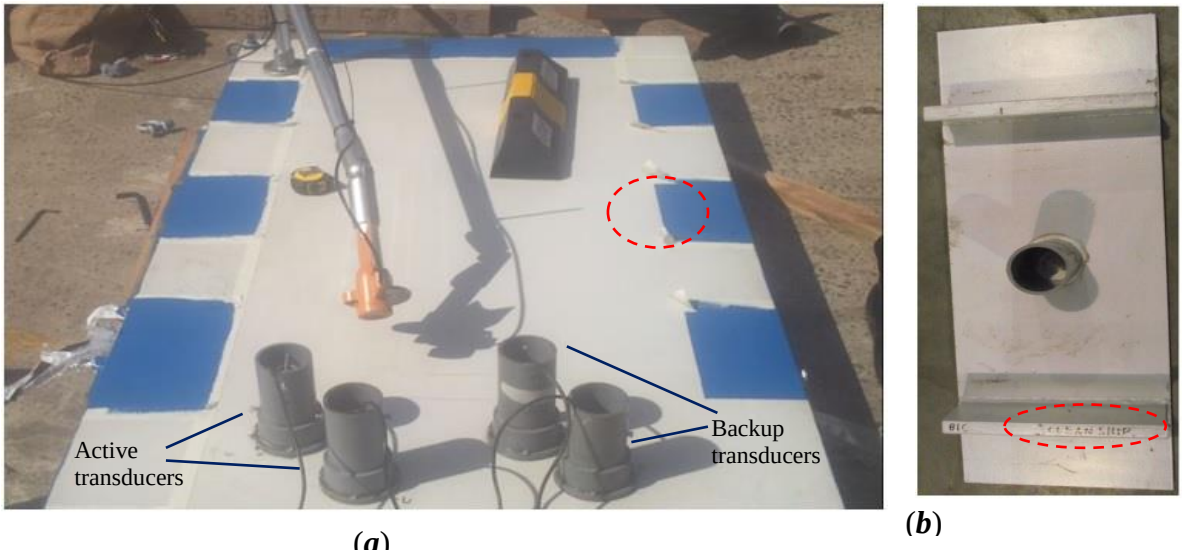

Figure 10: *a*) test set-up consisting of the plate coated by an anti-corrosion paint (white areas) and some patches coated by a copper-free anti-fouling paint (blue areas), likewise four transducers, and the underwater camera; b) control plate coated by anti-corrosion paint with no transducer used only as a control

The position of the array, the wave mode excited by the transducers and the operating frequency are selected according to the laboratory findings presented in the previous section. It is mentionable that some patches on the test plate (areas in blue in Fig.10*a*) were covered with a copper-free antifouling paint as an additional control. Moreover, an underwater camera was attached to the plate for monitoring its condition. The plates, as shown in Fig. 11, were then immersed in water at sufficient separation to deter the possibility that the ultrasonic waves on the test plate would be affecting the control plate.

The excitation frequency output was 47 kHz at which the Sofchem transducers had the most effective performance. The experiment was monitored remotely and the pictures taken from the plate by the underwater camera were transmitted to a laptop in the project office.

ISSN: 2454-1907
Impact Factor: 1.745 (I2OR)

Figure 11: Immersing the test plate in sea water

The plate status after 32 days in the water indicated no sign of fouling growth. Figure 13 displays a clear close-up photograph of part of the test plate, circled in dashed red in Fig. 10*a*, by the diver in which there is no sign of any type of fouling. On the contrary, Figs. 14 show two different parts of the control plate upon which fouling had already started to accumulate. Fig. 14b shows the part of the plate circled in red in Fig. 10b.

Comparing all the monitoring photographs of the control and test plates, it could be confidently inferred that the ultrasonic antifouling system has notable performance in antifouling and control of fouling growth using significantly low ultrasonic power levels.

Figure 13: A photograph of the test plate after 35 days in the water with no sign of fouling. This picture corresponds to the part circled in red in Fig.10*a*

ISSN: 2454-1907
Impact Factor: 1.745 (I2OR)

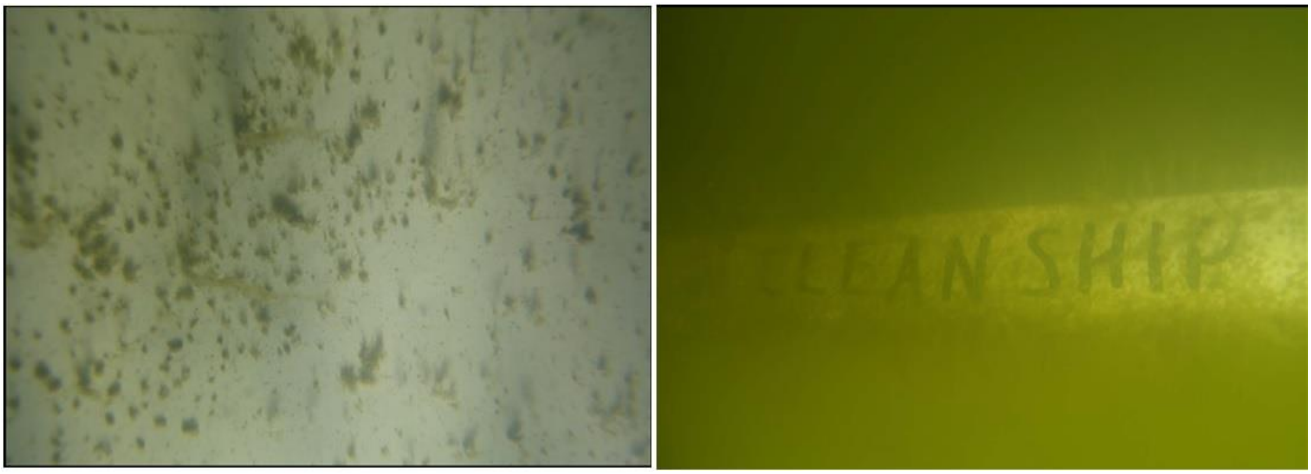

(*a*) (*b*)

Figure 14: Close-up photographs of the control plate after 34 days in water with biofouling growth; Fig.14b is corresponding to the part circled in red in Fig.10b.

This fact that the developed technique on its own is considerably effective in prevention, but ineffective in removal, implicitly indicates that the successful antifouling action of this approach is most likely not based on cavitation which destroys marine life. Rather it most probably relies on harmonic forces repelling the life types in a constant, gentle way which leads to the prevention of fouling accumulation.

4. CONCLUDING REMARKS

This work presented an experimental acoustic study for inhibiting the accretion of biofouling on a ship hull representative plate using UGWs. In this experiment, a large area of 2 m^2 was protected against fouling accumulation using just two commercially available transducers. In the light of efficiency, these types of wave propagate a long distance with only small attenuation and are thereby able to cover and protect much greater areas of the hull.

Selecting appropriate resonance frequencies for the transducers to exert a continuous, high frequency force perpendicular to the hull surface, as observed here in vibrometry analysis, causes a repelling mechanism to control biofouling without endangering sea life forms.

Finally, it must be noted that the study is a distinct work in terms of presenting an acoustic experiment well evidenced by in-situ photographs by both an underwater camera and by visual inspection by a human diver in a sea port environment. The work is one of the few sea trials ever performed and unlike most of acoustic studies carried out so far does not rely solely on limited laboratory results for specific type of fouling. Future work will focus on optimisation and performance indicators such as power and frequency with a view to scale up the field tests.

5. ACKNOWLEDGEMENTS

The research leading to these results has received funding from the European Union's Seventh Framework Programme managed by REA Research Executive Agency

http://ec.europa.eu/research/rea ([FP7/2007-2013]) for the project entitled "Prevention and detection of fouling on ship hulls" CLEANSHIP, under grant agreement no [312706], FP7-SME-2012-1 (http://cleanship-project.eu/). CLEANSHIP is collaboration between the following organisations: Brunel University, CERTH, Tecnalia, Enkon, Sofchem, WRS Marine, InnotecUK, and Lloyds's Register.

6. REFERENCES

[1] *Cao, S., Wang, J.D., Chen, H.S., et al., 2011, Progress of marine biofouling and antifouling technologies. Chinese Sci Bull, 56: 598–612, doi: 10.1007/s11434-010-4158-4.*

[2] *Olsen, S.M., 2009, Controlled release of environmentally friendly antifouling agents from marine coatings, Ph.D. dissertation, Department of Chemical and Biochemical Engineering, Technical University of Denmark.*

[3] *Champ M.A., 2000. A review of organotin regulatory strategies, pending actions, related costs and benefits. Sci Total Environ, 258: 21–71.*

[4] *Schultz, M.P., 2007. Effects of coating roughness and biofouling on ship resistance and powering. Biofouling 23(5), 331–341.*

[5] *Cooney J. J. and Tang R.-J., 1999. Quantifying effects of antifouling paints on microbial biofilm formation. Methods Enzymol 310: 637–645.*

[6] *Abbott A., Abel P.D., Arnold D.W., et al., 2000. Cost-benefit analysis of the use of TBT: The case for a treatment approach. Science of the total environment, 258: 5–19.*

[7] *Yebra, D.M., Kiil, S., Dam-Johansen, K., 2004. Antifouling technology-past, present and future steps towards efficient and environmentally friendly antifouling coatings. Prog. Org. Coat. 50(2), 75-104.*

[8] *Thomas, K., Brooks, S., 2010. The environmental fate and effects of antifouling paint biocides. Biofouling 26(1), 73–88.*

[9] *Mazue, G., Viennet, R., Hihn, J., Carpentier, L., Devidal, P., Albaina, I., 2011. Large-scale ultrasonic cleaning system: design of a multi-transducer device for boat cleaning (20 kHz). Ultrason. Sonochemistry 18(4), 895–900.*

[10] *Sheherbakov, P.S., Grigoryan, F.Y., Pogrebnyak, N.V., 1974. Distribution of high-frequency vibration in hulls of Krasnograd-class ships equipped with ultrasonic antifouling protection systems. In: Transaction. Technical Operations of the Maritime Fleet. Thermochemical Studies. Control of Corrosion and Fouling. No. AD 778380, February.*

[11] *Kitamura, H., Takahashi, K., Kanamaru, D., 1995. Inhibitory effect of ultrasonic waves on the larval settlement of the barnacle. Balanus amphitrite in the laboratory, Marinefouling 12(1), 9–13.*

[12] *Wilkens, S., Stanley, J., Jeffs, A., 2012. Induction of settlement in mussel (Perna canaliculus) larvae by vessel noise. Biofouling 28(1), 65–72.*

[13] *Gavand, M., McClintock, J., Amsler, C., Peters, R., Angus, R., 2007. Effects of sonication and advanced chemical oxidants on the unicellular green alga Dunaliella tertiolecta and cysts, larvae and adults of the brine shrimp Artemia salina: a prospective treatment to eradicate invasive organisms from ballast water. Mar. Pollut. Bull. 54(11),1777–1788.*

[14] *Choi, C., Scardino, A., Dylejko, P., Fletcher, L., Juniper, R., 2013. The effect of vibration frequency and amplitude on biofouling deterrence. Biofouling 29(2), 195–202.*

[15] Wartzok, D., Ketten, D.R., 1999. Marine mammal sensory systems. In: Biology of Marine Mammals, vol.1, pp.117–175.
[16] Stanley, J.A., Wilkens, S.L., Jeffs, A.G., 2014. Fouling in your own nest: vessel noise increases biofouling. Biofouling 30 (7), 837–844.
[17] Bott, T., 2000. Biofouling control with ultrasound. Heat Transf. Eng. 21(3), 43–49.
[18] Legg M., Yücel M.K., de Carellan I.G., Kappatos, V., Selcuk, C., Gan, T.H., 2015. Acoustic methods for biofouling control: A review. Ocean Engineering 103, 237–247.
[19] Rose, J.L., 1999. Ultrasonic Waves in Solid Media. Cambridge University Press.
[20] Svilainis L., Dumbrava V., Motiejunas G., 2008. Optimization of the ultrasonic excitation stage. in Information Technology Interfaces. ITI 2008, 30th International Conference on, pp. 791–796.